# Analysis of Rectangular Waveguide Discontinuities by the Method of Lines

Wilfrid Pascher, *Member, IEEE*, and Reinhold Pregla, *Senior Member*, IEEE

*Abstract*—**An efficient analysis of discontinuities in the rectangular waveguide is presented using the method of lines with one-dimensional discretization. As the line numbers in the incoming and outgoing waveguides are automatically correctly chosen in the method of lines, relative convergence is avoided. Scattering parameters for the $E$-plane step discontinuity are determined and an equivalent circuit for the diaphragm, the displacement, and a step with diaphragm is presented.**

## I. Introduction

Discontinuities in rectangular waveguides (Fig. 1) are commonly analyzed by the field expansion method [1], [2]. Another rigorous analysis technique, the method of lines, has been efficientlyapplied to various planar waveguide structures [3]–[17]. Apart from its numerical efficiency, one of the advantages of the method of lines is its easy formulation.

In this paper we apply the method of lines to rectangular waveguides discontinuities in the $E$-, or $H$-plane. We have to discretize the wave equation in one transverse direction only, since we use the known field behaviour in the other transverse direction. Posts and diaphragms have been already analysed in this way by Schulz [6], [7].

The $E$-plane step discontinuity (Fig. 2) is modelled using plain one-dimensional discretization. First the discretized coordinate is transformed to the spectral domain and an analytical solution is obtained for the longitudinal direction. In order to match the fields at the discontinuity we transform back to spatial domain. Finally the transmission and scattering matrices are computed from the incoming and outgoing waves. As the last two steps, namely the matching and the subsequent matrix analysis, differ from the other applications of the method of lines, these are treated in more detail in this paper. — The analysis of the displacement and the diaphragm is similar, but the fact that none of the waveguide cross sections is completely included in the other needs special consideration.

As examples for the applicability of the approach, the scattering parameters (or the equivalent circuits) for both the $E$-plane step discontinuity (with and without diaphragm) and the displacement (Fig. 1) are presented. In the following only $E$-plane discontinuities are investigated, since a generalisation to $H$-plane discontinuities is straightforward. Non-equidistant discretization can be incorporated easily.

Manuscript received January 13, 1993; revised May 9, 1994. The work reported in this paper was supported by a grant of the Deutsche Forschungsgemeinschaft.

The authors are with the Allgemeine und Theoretische Elektrotechnik, FernUniversität, Hagen, Germany.

IEEE Log Number 9407301

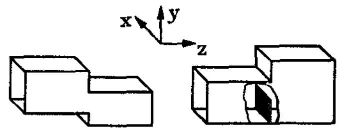


Fig. 1. Discontinuities in rectangular waveguides.

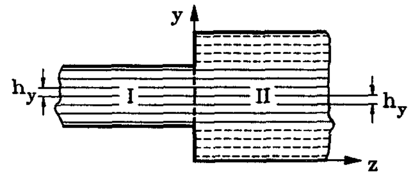


Fig. 2. Discretization of a step discontinuity.

## II. Field Equations for $E$-Plane Junctions

The only modes arising from the junctions of Fig. 1 by excitation with $TE_{10}$ to waves are $TE_{1n}$to $-X$ modes. The electromagnetic fields are derived from the potential

$$\mathbf{\Pi}_h = k_0^{-2}\psi \sin \bar{\lambda}_x \bar{x}\ \mathbf{a}_x$$

according to

$$\mathbf{E} = -jk_0 \nabla \times \mathbf{\Pi}_h$$
$$\eta_0 \mathbf{H} = \nabla \times \nabla \times \mathbf{\Pi}_h \qquad (1)$$

with a time dependence $\exp(j\omega t)$, the unit vector $\mathbf{a}_x$ and $\bar{\lambda}_x = \pi/\bar{a}$. The waveguide width $a$ is assumed to be constant for the whole structure, and the coordinates and lengths are normalized by $\bar{x} = k_0 x$ etc.

The transverse field components run

$$\begin{array}{ll} E_x = 0 & \eta_0 H_x = (\varepsilon_r - \bar{\lambda}_x^2) \sin \bar{\lambda}_x \bar{x} \cdot \psi \\ E_y - j \sin \bar{\lambda}_x \bar{x} \cdot \frac{\partial \psi}{\partial \bar{z}} & \eta_0 H_y = \bar{\lambda}_x \cos \bar{\lambda}_x \bar{x} \cdot \frac{\partial \psi}{\partial \bar{y}} \end{array} \qquad (2)$$

The potential $\psi$ must fulfill the Neumann condition at all metallic boundaries.

## III. Modelling of a Step Discontinuity

Using the above field equations the waveguide step shown in Fig. 2 is analyzed. Discretization and transformation of the scalar potential are performed as usual in the method of lines [3], [4].

### A. First Step: Discretization of the Wave Equation

Both waveguides (Region I, II) are discretized with the same discretization distance $h_y$. Different line numbers $N_{\mathrm{I}}$ and $N_{\mathrm{II}}$ result, which are approximately proportional to the waveguide heights. As the mode numbers $M_i$ are equal to the line numbers $N_\imath$, the criterion to avoid relative convergence after *Mittra et al.* [8]

$$M_2/M_1 = b_2/b_1 \tag{3}$$

is fulfilled naturally in the MoL.

We discretize the Helmholtz equation

$$\frac{\partial^2\psi}{\partial\bar{z}^2} + \frac{\partial^2\psi}{\partial\bar{y}^2} - \bar{\lambda}_x^2\psi + \varepsilon_r\psi = 0 \tag{4}$$

using the following finite difference expression for the second derivative

$$\left.\frac{\partial^2\psi}{\partial\bar{y}^2}\right|_i \approx \frac{\psi_{i+1} - 2\psi_i + \psi_{i-1}}{\bar{h}_y^2} \longrightarrow (\bar{h}_y)^{-2}\mathbf{D}_{yy}\boldsymbol{\psi} \tag{5}$$

to obtain

$$\frac{d^2\boldsymbol{\psi}}{d\bar{z}^2} - (\bar{\lambda}_x^2\mathbf{I} - (\bar{h}_y)^{-2}\mathbf{D}_{yy} - \varepsilon_r\mathbf{I})\boldsymbol{\psi} = \mathbf{0} \tag{6}$$

The difference operator $\mathbf{D}_{yy}$ has different sizes $N_{\mathrm{I}}$ and $N_{\mathrm{II}}$ in the two regions. As $\mathbf{D}_{yy}$ is a tridiagonal matrix, the discretized wave equation (6) is a system of **coupled ordinary equations** for the discretized potential $\boldsymbol{\psi}$.

### *B. Second Step: Transformation of the Potentials*

We transform to diagonal form by

$$\left(\bar{h}_y\right)^{-2}\mathbf{T}^t\mathbf{D}_{yy}\mathbf{T} = -\bar{\boldsymbol{\lambda}}_y^2 \tag{7}$$

where $t$ denotes transpose. The transformation matrices $\mathbf{T}_{\mathrm{I,II}}$ and the eigenvalue matrices $\bar{\boldsymbol{\lambda}}_y^{\mathrm{I,II}}$ are different for the two waveguides. The difference operators $\mathbf{D}_{yy}$ and the transformation matrices $\mathbf{T}$ are calculated according to the Neumann boundary conditions on both side walls [4].

We transform the discretized wave (6) and obtain a system of **uncoupled ordinary differential equations**

$$\frac{d^2\bar{\boldsymbol{\psi}}}{d\bar{z}^2} - \underbrace{\left(\bar{\boldsymbol{\lambda}}_x^2\mathbf{I} + \bar{\boldsymbol{\lambda}}_y^2 - \varepsilon_r\mathbf{I}\right)}_{\boldsymbol{\Gamma}^2}\bar{\boldsymbol{\psi}} = \mathbf{0} \tag{8}$$

for the transformed potential $\bar{\boldsymbol{\psi}} = \mathbf{T}^t\boldsymbol{\psi}$ with the propagation constants $\boldsymbol{\Gamma}$, which are diagonal matrices.

The transformed potentials result as the **solutions of the wave equation** (8):

| **Waveguide I** | **Waveguide II** |
|---|---|
| $\bar{\boldsymbol{\psi}}^{\mathrm{I}} = e^{-\boldsymbol{\Gamma}_{\mathrm{I}}\bar{z}}\mathbf{A}^{\mathrm{I}} + e^{\boldsymbol{\Gamma}_{\mathrm{I}}\bar{z}}\mathbf{B}^{\mathrm{I}}$ | $\bar{\boldsymbol{\psi}}^{\mathrm{II}} = e^{\boldsymbol{\Gamma}_{\mathrm{II}}\bar{z}}\mathbf{A}^{\mathrm{II}} + e^{-\boldsymbol{\Gamma}_{\mathrm{II}}\bar{z}}\mathbf{B}^{\mathrm{II}}$ |

### *C. Third Step: Field Matching at the Step $z = 0$*

The transverse field components $E_y$ and $H_x$, that means $\psi$ and $\partial\psi/\partial\bar{z}$ must be matched. If $\psi$ is matched on all the discretization lines, $\partial\psi/\partial\bar{y}$ and thus $H_y$ is also matched. In the transform domain we obtain at $z = 0$

$$\bar{\boldsymbol{\psi}}^{\mathrm{I}} = \mathbf{A}^{\mathrm{I}} + \mathbf{B}^{\mathrm{I}} \qquad \bar{\boldsymbol{\psi}}^{\mathrm{II}} = \mathbf{A}^{\mathrm{II}} + \mathbf{B}^{\mathrm{II}}$$

$$\frac{\partial\bar{\boldsymbol{\psi}}^{\mathrm{I}}}{\partial\bar{z}} = -\boldsymbol{\Gamma}_{\mathrm{I}}(\mathbf{A}^{\mathrm{I}} - \mathbf{B}^{\mathrm{I}}) \qquad \frac{\partial\bar{\boldsymbol{\psi}}^{\mathrm{II}}}{\partial\bar{z}} = \boldsymbol{\Gamma}_{\mathrm{II}}(\mathbf{A}^{\mathrm{II}} - \mathbf{B}^{\mathrm{II}})$$

In the vectors $\mathbf{A}^{\mathrm{I}}$ and $\mathbf{A}^{\mathrm{II}}$ only the first element is non-zero for excitation with the fundamental mode.

The matching has to be achieved in *spatial domain* after the inverse transformation. To this end we partition the transformation matrix $\mathbf{T}_{\mathrm{II}}$ into two submatrices

$$\mathbf{T}_{\mathrm{II}} = \begin{bmatrix}\mathbf{T}_{\mathrm{II}}^r \\ \mathbf{T}_{\mathrm{II}}^c\end{bmatrix} \tag{9}$$

$\mathbf{T}_{\mathrm{II}}^r$ corresponds to the aperture part of waveguide $II$ opposite waveguide I (full lines in Fig. 2) and hence has the same number of rows $N_{\mathrm{II}}^r = N_{\mathrm{I}}$ as $\mathbf{T}_{\mathrm{I}}$. $\mathbf{T}_{\mathrm{II}}^c$ corresponds to the front plate (broken lines in Fig. 2) with $N_{\mathrm{II}}^c = N_{\mathrm{II}} - N_{\mathrm{I}}$

The two matching steps are

1) Matching of $H_x$, that means of $\psi$, as the factor $(\varepsilon_r - \bar{\lambda}_x^2)\sin\bar{\lambda}_x\bar{x}$ (see (2)) is the same for both waveguides and for all components of $H_x$. This yields

$$\mathbf{T}_{\mathrm{I}}(\mathbf{A}^{\mathrm{I}} + \mathbf{B}^{\mathrm{I}}) = \mathbf{T}_{\mathrm{II}}^{\mathbf{r}}(\mathbf{A}^{\mathrm{II}} + \mathbf{B}^{\mathrm{II}}) \tag{10}$$

2) Matching of $E_y$, that means of $\frac{\partial\boldsymbol{\psi}}{\partial\bar{z}}$ (see (2)), yields

in the aperture I-II

$$-\mathbf{T}_{\mathrm{I}}\boldsymbol{\Gamma}_{\mathrm{I}}(\mathbf{A}^{\mathrm{I}} - \mathbf{B}^{\mathrm{I}}) = \mathbf{T}_{\mathrm{II}}^r\boldsymbol{\Gamma}_{\mathrm{II}}(\mathbf{A}^{\mathrm{II}} - \mathbf{B}^{\mathrm{II}}) \tag{11}$$

on the front plate II

$$\mathbf{0} = \mathbf{T}_{\mathrm{II}}^c\boldsymbol{\Gamma}_{\mathrm{II}}(\mathbf{A}^{\mathrm{II}} - \mathbf{B}^{\mathrm{II}}) \tag{12}$$

### *D. Transmission Matrix and Scattering Matrix*

For the calculation of the **transmission matrix** we combine the matching equations (10), (11) to the following system

$$\mathbf{A}^{\mathrm{I}} + \mathbf{B}^{\mathrm{I}} = \mathbf{T}(\mathbf{B}^{\mathrm{II}} + \mathbf{A}^{\mathrm{II}}) \tag{13}$$

$$\mathbf{A}^{\mathrm{I}} - \mathbf{B}^{\mathrm{I}} = \boldsymbol{\Gamma}_{\mathrm{I}}^{-1}\mathbf{T}\boldsymbol{\Gamma}_{\mathrm{II}}(\mathbf{B}^{\mathrm{II}} - \mathbf{A}^{\mathrm{II}}) \tag{14}$$

with the abbreviation $\mathbf{T} = \mathbf{T}_{\mathrm{I}}^t\mathbf{T}_{\mathrm{II}}^r$ (see App.). We solve this system of equations for the wave coefficients in the smaller waveguide I. With (12) we obtain the transmission matrix equation

$$\begin{bmatrix}\mathbf{A}^{\mathrm{I}} \\ \mathbf{0} \\ \hline \mathbf{B}^{\mathrm{I}}\end{bmatrix} = \begin{bmatrix}\tilde{\mathbf{T}}_+ & \tilde{\mathbf{T}}_- \\ \mathbf{T}_{\mathrm{II}}^c\boldsymbol{\Gamma}_{\mathrm{II}} & -\mathbf{T}_{\mathrm{II}}^c\boldsymbol{\Gamma}_{\mathrm{II}} \\ \hline \tilde{\mathbf{T}}_- & \tilde{\mathbf{T}}_+\end{bmatrix}\begin{bmatrix}\mathbf{B}^{\mathrm{II}} \\ \mathbf{A}^{\mathrm{II}}\end{bmatrix} \tag{15}$$

with the submatrices

$$\tilde{\mathbf{T}}_\pm = \frac{1}{2}(\mathbf{T} \pm \boldsymbol{\Gamma}_{\mathrm{I}}^{-1}\mathbf{T}\boldsymbol{\Gamma}_{\mathrm{II}}) \tag{16}$$

Using (15) the incoming and outgoing waves at the smaller waveguide I are computed from the incoming and outgoing waves at the larger waveguide II. To compute the waves reversely, namely from the smaller waveguide I to the larger II, is only possible with $N_{\mathrm{II}} - N_{\mathrm{I}}$ additional equations. An alternative way is to use the scattering matrix.

For the calculation of the **scattering matrix** we solve the transmission matrix (15) for $\mathbf{B}^{\mathrm{I}}$ and $\mathbf{B}^{\mathrm{II}}$. For the amplitudes of the outgoing waves we obtain

$$\mathbf{B}^{\mathrm{II}} = \begin{bmatrix}\tilde{\mathbf{T}}_+ \\ \mathbf{T}_{\mathrm{II}}^c\boldsymbol{\Gamma}_{\mathrm{II}}\end{bmatrix}^{-1}\begin{bmatrix}\mathbf{I} & -\tilde{\mathbf{T}}_- \\ \mathbf{0} & +\mathbf{T}_{\mathrm{II}}^c\boldsymbol{\Gamma}_{\mathrm{II}}\end{bmatrix}\begin{bmatrix}\mathbf{A}^{\mathrm{I}} \\ \mathbf{A}^{\mathrm{II}}\end{bmatrix} \tag{17}$$

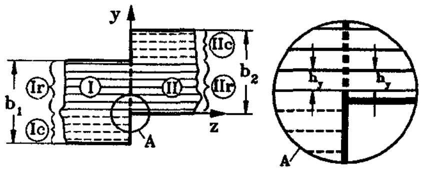


Fig. 3. Discretization of a displacement.

$\mathbf{B}^{\mathrm{I}}$ is computed from the last line of (15).
For the calculation of the **scattering matrix for the fundamental modes,** which is defined according to

$$\begin{bmatrix} B_1^{\mathrm{I}} \\ B_1^{\mathrm{II}} \end{bmatrix} = \begin{bmatrix} S_{11} & S_{12} \\ S_{21} & S_{22} \end{bmatrix} \begin{bmatrix} A_1^{\mathrm{I}} \\ A_1^{\mathrm{II}} \end{bmatrix} \tag{18}$$

we set the excitations $A_1^{\mathrm{I}}$ and $A_1^{\mathrm{II}}$ to zero individually.

## IV. Modifications for Displacement and Diaphragm

In the case of a diaphragm or a displacement, (Fig. 3) none of the two waveguides is completely included in the other one. This is the only difference to the step discontinuity, hence the analysis runs as above with the following modifications. We have to distinguish an aperture region (full lines) and an additional front plate (broken lines) also for the waveguide I in contrast to the step discontinuity (Fig. 2).

Hence we have to partition the transformation matrix $\mathbf{T}_{\mathrm{I}}$ as well:

$$\mathbf{T}_{\mathrm{I}} = \begin{bmatrix} \mathbf{T}_{\mathrm{I}}^{r} \\ \mathbf{T}_{\mathrm{I}}^{c} \end{bmatrix} \tag{19}$$

with $\mathbf{T}_{\mathrm{I}}^{r}$ for the aperture and $\mathbf{T}_{\mathrm{I}}^{c}$ for the front plate. This results in two changes in the analysis. First we replace $\mathbf{T}_{\mathrm{I}}$ by $\mathbf{T}_{\mathrm{I}}^{r}$ in matching equations (10) to (12) and second we obtain the additional equation

$$\text{on the front plate I} \qquad \mathbf{T}_{\mathrm{I}}^{c}\mathbf{\Gamma}_{\mathrm{I}}(\mathbf{A}^{\mathrm{I}} - \mathbf{B}^{\mathrm{I}}) = \mathbf{0} \tag{20}$$

Equation (14) is still valid, if $\mathbf{T}$ is replaced by $\mathbf{T}' = \mathbf{T}_{\mathrm{I}}^{rt}\mathbf{T}_{\mathrm{II}}^{r}$. But the equation corresponding to (10) cannot be converted into the form of (13) any more, as $\mathbf{T}_{\mathrm{I}}^{r}$ itself is not invertible. The number of equations for $\mathbf{A}^{\mathrm{I}}$ and $\mathbf{B}^{\mathrm{I}}$ is no longer sufficient to calculate the transmission matrix.

We are still able to determine the **scattering matrix**, however, in an analogous way as above.
With

$$\hat{\mathbf{T}}' = \mathbf{\Gamma}_{\mathrm{I}}^{-1}\mathbf{T}'\mathbf{\Gamma}_{\mathrm{II}}$$

and the following substitution

$$\tilde{\mathbf{T}}_{\pm} \longrightarrow \tilde{\mathbf{T}}'_{\pm} = \frac{1}{2}(\mathbf{T}_{\mathrm{II}}^{r} \pm \mathbf{T}_{\mathrm{I}}^{r}\mathbf{\Gamma}_{\mathrm{I}}^{-1}\mathbf{T}'\mathbf{\Gamma}_{\mathrm{II}})$$

which considers $\mathbf{T}_{\mathrm{I}}^{r}$ as an additional factor, we obtain by reordering of (14) and from the first line of (15):

$$\left[\begin{array}{cc} \mathbf{I} & \hat{\mathbf{T}}' \\ \hline \mathbf{0} & \tilde{\mathbf{T}}'_{+} \\ \mathbf{0} & \mathbf{T}_{\mathrm{II}}^{c}\mathbf{\Gamma}_{\mathrm{II}} \end{array}\right] \begin{bmatrix} \mathbf{B}^{\mathrm{I}} \\ \mathbf{B}^{\mathrm{II}} \end{bmatrix} = \left[\begin{array}{cc} \mathbf{I} & \hat{\mathbf{T}}' \\ \hline \mathbf{T}_{\mathrm{I}}^{r} & -\tilde{\mathbf{T}}'_{-} \\ \mathbf{0} & +\mathbf{T}_{\mathrm{II}}^{c}\mathbf{\Gamma}_{\mathrm{II}} \end{array}\right] \begin{bmatrix} \mathbf{A}^{\mathrm{I}} \\ \mathbf{A}^{\mathrm{II}} \end{bmatrix} \tag{21}$$

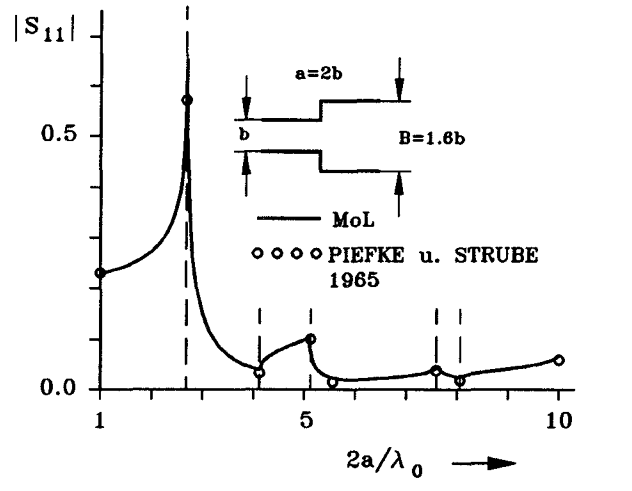


Fig. 4. Symmetric $E$-plane step discontinuity. Magnitude of the reflection coefficient as a function of normalized frequency. Cut-off frequencies are marked. With free space wavelength $\lambda_0$. o o o MMT [1].

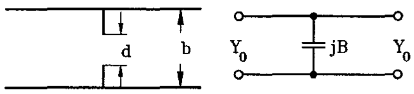


Fig. 5. Side view and equivalent circuit of a diaphragm.

Thus the amplitudes of the outgoing waves are given by:

$$\mathbf{B}^{\mathrm{II}} = \begin{bmatrix} \tilde{\mathbf{T}}'_{+} \\ \mathbf{T}_{\mathrm{II}}^{c}\mathbf{\Gamma}_{\mathrm{II}} \end{bmatrix}^{-1} \begin{bmatrix} \mathbf{T}_{\mathrm{I}}^{r} & -\tilde{\mathbf{T}}'_{-} \\ \mathbf{0} & +\mathbf{T}_{\mathrm{II}}^{c}\mathbf{\Gamma}_{\mathrm{II}} \end{bmatrix} \begin{bmatrix} \mathbf{A}^{\mathrm{I}} \\ \mathbf{A}^{\mathrm{II}} \end{bmatrix} \tag{22}$$

$\mathbf{B}^{\mathrm{I}}$ is computed from the first line of (21) and the scattering matrix of the fundamental modes ist determined by relation (18) again.

## V. Results

The scattering parameters or the resulting equivalent circuit parameters for various discontinuities are presented and compared with results from literature. For the symmetric $E$-plane step discontinuity the magnitude of the reflection coefficient is given in Fig. 4 as a function of normalized frequency. The agreement with the mode matching technique (MMT) [1] is good, even for the marked values of the cut-off frequencies.

The next three structures are analyzed with the approach of Section IV. For the step discontinuity with diaphragm in a parallel plate wavegude (Fig. 7) the junction susceptance $B$ normalized with respect to the TEM admittance $Y_1^0$ of the first waveguide is given by

$$j\bar{B} = j\frac{B}{Y_1^0} = \frac{1 + S_{11}}{1 - S_{11}} - \frac{Y_2^0}{Y_1^0}\frac{b_1}{b_2}$$

This formula is also valid for the diaphragm alone (Fig. 5). The results in Fig. 6 are in very good agreement with Marcuvitz [8].

In Fig. 7 the normalized susceptance of a step with a diaphragm is compared with results from the conservation of

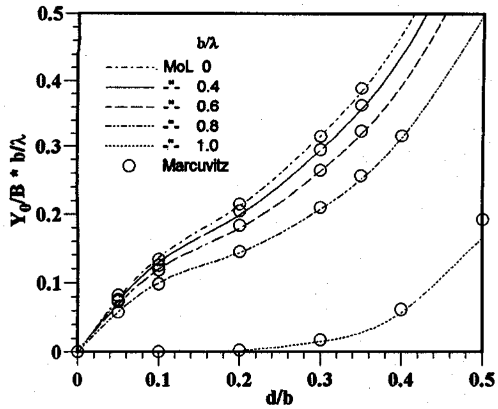


Fig. 6. Susceptance of a diaphragm in a rectangular waveguide. + + + [9].

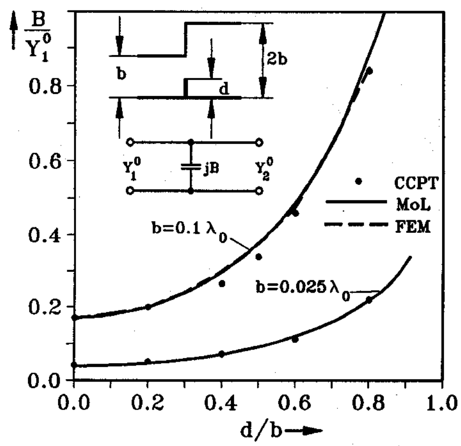


Fig. 7. Step with a diaphragm in a parallel plate waveguide. Normalized susceptance $\bar{B}$ versus diaphragm height. •[10]– – –[11].

complex power technique (CCPT) [10] and the finite element method (FEM) [11]. The deviation of two data points from the CCPT is probably due to a distortion in the diagram in [10].

In Table I excellent agreement (better than 0.04%) is found with the MMT [2] for the shunt reactance of a displacement (Fig. 8). These results were obtained for an average line number $n' = 50$ in the discontinuity corresponding to [2]. Thus the convergence of the method of lines is very good.

## VI. Conclusion

The principles of the $E$-plane junction analysis by the MoL, are demonstrated. The modelling of a step discontinuity leads to simple matrix equations, which are extended to displacements and diaphragms in a straightforward manner. As the line numbers in different waveguides are always chosen correctly in the MoL, relative convergence is automatically avoided. The equivalent circuit parameters of the above mentioned discontinuities, and of the combination of step discontinuity and diaphragm, agree very well with literature.

## Appendix Transformation Matrices and Characteristic Values for the Waveguide Step

The product of the transformation matrices $\mathbf{T}_{\mathrm{I}}^{t}$ and $\mathbf{T}_{\mathrm{II}}^{r}$ yields:

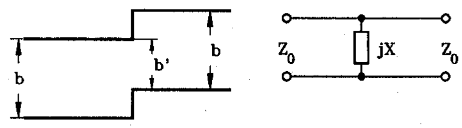


Fig. 8. Side view and equivalent circuit of a displacement.

TABLE I
Normalized Shunt Reactance $X/Z_0 \cdot b/\lambda_g$ of an $E$–Plane Offset in Terms of normalized Frequency $2b/\lambda_g$ and Fractional Displacement $b'/b$
Upper Values: MoL; Lower Values: MMT [2]

| $-\frac{X}{Z_0} \cdot \frac{b}{\lambda_g}$ | | $2b/\lambda_g$ | | | |
|---|---|---|---|---|---|
| | | 0.2 | 0.4 | 0.6 | 0.8 |
| $b'/b$ | 0.1 | 0.063422 | 0.061026 | 0.056362 | 0.047273 |
| | | 0.063407 | 0.061017 | 0.056353 | 0.047260 |
| | 0.3 | 0.14057 | 0.13272 | 0.11799 | 0.091598 |
| | | 0.14058 | 0.13270 | 0.11795 | 0.091599 |
| | 0.5 | 0.29767 | 0.27957 | 0.24607 | 0.18768 |
| | | 0.29769 | 0.27961 | 0.24608 | 0.18772 |
| | 0.7 | 0.79752 | 0.75734 | 0.67323 | 0.52797 |
| | | 0.79744 | 0.75423 | 0.67308 | 0.52786 |
| | 0.9 | 5.8077 | 5.5943 | 5.1707 | 4.3350 |
| | | 5.8069 | 5.5926 | 5.1699 | 4.3343 |

$$\mathbf{T}_{ik} = \frac{1}{2}\sqrt{\frac{(2-\delta_{i0})(2-\delta_{k0})}{N_{\mathrm{I}}N_{\mathrm{II}}}} \times \sum_{l=0}^{N_{\mathrm{I}}-1} (\cos(\alpha_{il}+\beta_{kl}) - \cos(\alpha_{il}-\beta_{kl})) \tag{23}$$

with

$$\alpha_{il} = \left(l + \frac{1}{2}\right)\frac{i\pi}{N_{\mathrm{I}}} \qquad (i = 0 \cdots N_{\mathrm{I}} - 1)$$

$$\beta_{kl} = \left(l + \frac{1}{2} + N_s\right)\frac{k\pi}{N_{\mathrm{II}}} \qquad (k = 0 \cdots N_{\mathrm{II}} - 1)$$

The characteristic values run for $NN$ boundaries

$$\bar{\lambda}_{yi} = \bar{h}_y^{-1} \sin\frac{i\pi}{2N} \tag{24}$$

## REFERENCES

[1] G. Piefke and R. Strube, "Reflexion und Transmission bei Einfall einer $H_{10}$-Welle auf eine sprunghafte Änderung eines Rechteckhohlleiters in der $E$-Ebene," *Arch. Elektron. Übertragungstech., AEÜ 19*, pp. 231–243, 1965.

[2] E. Kühn, "Microwave bandpass filters consisting of rectangular waveguides with 1-dimensional offsets," *Circuit Theory Appl., 6*, pp. 13–29, 1978.

[3] U. Schulz and R. Pregla, "A new technique for the analysis of the dispersion characteristics of planar wavequides," *Arch. Elektron.Übertragungstech., AEÜ 34*, pp. 169–173, 1980.

[4] R. Pregla and W. Pascher, "The Method of Lines," in *Numerical Techniques for Microwave and Millimeter Wave Passive Structures* T. Itoh, Ed. New York: Wiley, 1989, pp. 381–446.

[5] R. Pregla, "Analysis of a bend discontinuity by the method of lines," *Frequenz, 45*, pp. 213–216, 1991.

[6] U. Schulz, "The Method of Lines—A New Technique for the Analysis of Planar Microwave Structures," (in German), *Ph.D. thesis*, FernUniv., Hagen, Federal Republic of Germany, 1980.

[7] ——, "Evaluation of the equivalent circuit parameters of posts and diaphragms in waveguides by the method of lines" (in German), *Arch. Elektron. Übertragungstech., AEÜ 39*, pp. 203–207, 1985.

[8] R. Mittra, T. Itoh, and T. Li, "Analytical and numerical studies of the relative convergence phenomenon arising in the solution of an integral equation by the moment method," *IEEE Trans. Microwave Theory Tech.*, vol. MTT-20, pp. 96–104, 1972.

[9] N. Marcuvitz, *Waveguide Handbook* London: Peregrinus Ltd., 1986, pp. 218–221.

[10] E. M. Sich and R. H. Macphie, "The conservation of complex power technique and $E$-plane step-diaphragm junction discontinuities," *IEEE Trans. Microwave Theory Tech.*, vol. MTT-30, pp. 198–201, 1982.

[11] M. Koshiba *et al.*, "Application of finite-element method to $E$-plane waveguide discontinuities," *Trans. IECE (Japan), E66*, pp. 457–458, 1983.

**Wilfrid Pascher** was born in Graz, Austria, on September 17, 1958. He received his master's degree in Technical Physics (Dipl.-Ing.) from the Technical University Graz and the doctorate of engineering (Dr.-Ing.) from the FernUniversität in Hagen, in 1984 and 1990, respectively.

From 1985 to 1990 he was a research assistant in the Department of Electrical Engineering of the FernUniversität, where he was engaged in the investigation of planar and rectangular waveguide components. Since 1990 he has been a senior engineer and is currently involved in the numerical modelling of passive components for integrated optics.

**Reinhold Pregla** (M'76-SM'83) received the master's degree in electrical engineering (Dipl.-Ing.) and the doctorate engineering (Dr.-Ing.) from the Technische Universität Braunschweig, West Germany, in 1963 and 1966, respectively.

From 1966 to 1969 he was a research assistant in the Department of Electrical Engineering of the Technische Universität Braunschweig (Institut für Hochfrequenztechnik), where he was engaged in investigations of microwave filters. After the Habilitation, he was a lecturer in high frequencies at the Technische Universität Braunschweig. Since 1973 he has held the position of professor at the Ruhr-Universität Bochum, West Germany, and since 1975, he has held the position of full professor in electrical engineering at the FernUniversität (a university for distance study) in Hagen, West Germany. His fields of investigation include microwave passive circuits, waveguide theory for microwaves and optics, antennas, and laser modelling.